A search for intermediate-mass black holes mergers in the second LIGO–Virgo observing run with the Bayes Coherence Ratio

Avi Vajpeyi,[1,2,*] Rory Smith,[1,2] Eric Thrane,[1,2] Gregory Ashton,[1,2,3] Thomas Alford,[4] Sierra Garza,[4] Maximiliano Isi,[5,6] Jonah Kanner,[4] T. J. Massinger,[4] and Liting Xiao[4]

[1]*School of Physics and Astronomy, Monash University, Clayton VIC 3800, Australia*
[2]*OzGrav: The ARC Centre of Excellence for Gravitational Wave Discovery, Clayton VIC 3800, Australia*
[3]*Department of Physics, Royal Holloway, University of London, TW20 0EX, United Kingdom*
[4]*LIGO Laboratory, California Institute of Technology, Pasadena, CA 91125, USA*
[5]*LIGO Laboratory, Massachusetts Institute of Technology, Cambridge, MA 02139, USA*
[6]*Department of Physics and Kavli Institute for Astrophysics and Space Research, Massachusetts Institute of Technology, 77 Massachusetts Ave, Cambridge, MA 02139, USA*

(Dated: August 4, 2021)

The detection of an intermediate-mass black hole population ($10^2 - 10^6\ M_\odot$) will provide clues to their formation environments (e.g., disks of active galactic nuclei, globular clusters) and illuminate a potential pathway to produce supermassive black holes. Ground-based gravitational-wave detectors are sensitive to a subset of such mergers and have been used to detect one $142^{+28}_{-16}\ M_\odot$ intermediate-mass black hole formation event. However, ground-based detector data contain numerous incoherent short duration noise transients that can mimic the gravitational-wave signals from merging intermediate-mass black holes, limiting the sensitivity of searches. Here we search for binary black hole mergers using a Bayesian-inspired ranking statistic which measures the coherence or incoherence of triggers in multiple-detector data. We use this statistic to identify candidate events with lab-frame total masses $\gtrsim 55\ M_\odot$ using data from LIGO's second observing run. Our analysis does not yield evidence for new intermediate-mass black holes. However, we find support for some stellar-mass binary black holes not reported in the first LIGO–Virgo gravitational-wave transient catalog, GWTC-1.

I. INTRODUCTION

A variety of techniques have been employed to search for $10^4 - 10^6\ M_\odot$ intermediate-mass black hole (IMBH) candidates including reverberation mapping [1], direct kinematic measurements [2, 3], applying macroscopic galaxy to black hole mass scaling relations (M_{BH}-σ and M_{BH}-L relations) [4, 5], studying X-ray luminosity and spectra [6, 7], gravitational lensing of gamma-ray burst light curves [8], and others [9–11]). However, because IMBH have smaller gravitational spheres of influence than those of supermassive black holes, it is much more challenging to observe them with these observational techniques [11]. Additionally, the numerous IMBH candidates discovered using these techniques are ambiguous as other sources can describe observations from the candidates (e.g., light sources orbiting clusters of stellar-mass black holes [12, 13], anisotropic emission from neutron stars [14, 15]).

Stellar mass ($M_{\rm BH} < 10^2\ M_\odot$) and supermassive black holes ($M_{\rm BH} > 10^6\ M_\odot$) have been observed and well studied since the 1970s [16–22]. However, there is a deficiency of observational evidence for black holes in the intermediate-mass range $10^2 - 10^6\ M_\odot$. The discovery of an IMBH population will bridge this observational gap, probe IMBH formation environments (e.g. accretion disks of active galactic nuclei [23–35], the centers of dense stellar clusters [36–46], Population-III stars [47–51]), and illuminate our understanding of supermassive black hole formation [52–55].

Compact binary coalescences (CBCs) can provide unambiguous gravitational-wave signals for IMBH candidates e.g., the $142^{+28}_{-16}\ M_\odot$ (90% credible intervals) remnant observed from the gravitational-wave event GW190521 [56] and other candidates [57–59]. As a binary's total mass M_T is associated with its gravitational-wave merger frequency, $f \sim M_T^{-1}$, ground-based gravitational-wave detectors ($f \sim 10^1 - 10^3$ Hz) are sensitive to the last milliseconds of merging systems with $100\ M_\odot < M_T^{\rm lab} < 400\ M_\odot$ [60–63], while space-based detectors ($f \sim 10^{-2} - 10^1$ Hz) can study the full signals of merging systems with $10^4\ M_\odot < M_T^{\rm lab} < 10^7\ M_\odot$ [62, 64]. Because of the short duration of IMBH gravitational-wave signals in ground-based detectors, data quality is critical for their detection. Gravitational-wave data is characterized by numerous non-stationary terrestrial artifacts called *glitches* [65–67]. Like signals from IMBH mergers, most glitches last for a fraction of a second, making them difficult to distinguish from astrophysical signals. These glitches can decrease the sensitivity of searches for binary black hole mergers with $M_T^{\rm lab} \gtrsim 55\ M_\odot$ [65].

Although a significant fraction of the glitches can be identified by testing them for coherence amongst two or more detectors and performing matched-filtering, these methods are insufficient to identify all glitches [65–67]. One method to discriminate more glitches while searching for CBCs is the Bayesian odds [68–73]. The Bayesian

* avi.vajpeyi@monash.edu

Coherence Ratio $\rho_{\rm BCR}$ [70, 71] is a Bayesian odds comparing the probability that the data contains coherent signals vs. incoherent glitches. In this paper, we use the $\rho_{\rm BCR}$ to rank O2's coincident CBC gravitational-wave candidates with lab-frame total masses in the range of $55-500\,M_\odot$. We present the candidates' $p_{\rm S}$, the probability that the candidate originates from a coherent gravitational-wave source. Additionally, for comparison, we provide the candidate's $p_{\rm astro}$ values reported by the LIGO-Virgo-KAGRA (LVK) collaboration in GWTC-1 [74], the PyCBC-team [75–84], by the Institute of Advanced study's team (IAS) [85–87], and by Pratten and Vecchio [73].

We find that (a) events reported in GWTC-1, including GW170729 (likely the most massive BBH system in GWTC-1) are statistically significant $p_{\rm S} > 0.9$; (b) three out of the eight IAS events and candidates have $p_{\rm S} > 0.9$, corroborating IAS's detection claims for GW170304, GW170727, and GW170817A; and that (c) our ranking statistic does not identify any new IMBH, but does identify an unreported marginal stellar-mass binary black hole candidate, 170222[1] with $p_{\rm S} \sim 0.6$.

The remainder of this paper is structured as follows. We outline our methods, including details of our ranking statistic and the retrieval of our candidates in Section II. We present details on the implementation of our analysis in Section III. Finally, we present our results in Section IV and discuss these results in the context of the significance of gravitational-wave candidates in Section V.

II. METHOD

A. A Bayesian Ranking Statistic

The standard framework to identify CBC gravitational-wave signals in data is to quantify the significance of candidates with null-hypothesis significance testing [74, 88]. In this framework, the candidates' ranking statistic is compared against a background distribution. The independent matched-filter searches, e.g., PyCBC [80], SPIIR [89] and GstLAL [90], and Coherent WaveBurst [91] used by LVK to search for signals in gravitational-wave data all use ranking statistics in such a manner [74]. Both PyCBC and GstLAL's ranking statistic incorporate information about the relative likelihood that the data contains a coherent signal versus noise. In contrast, cWB's ranking statistic uses the information of coherent energy present in the network of detectors [74].

Bayesian inference offers an alternative means to rank the significance of candidate events by computing the odds that the data contain a transient gravitational-wave signal versus instrumental glitches [70]. This method relies on accurate models for the signal and glitch morphologies [70]. In principle, Bayesian odds is the optimal method for hypothesis testing [71]. Much of its power comes from the Bayesian evidence, the likelihood of the data given a hypothesis. However, the evidence is not used in current matched filter searches. Here, we explore a hybrid frequentist/Bayesian ranking statistic that makes use of the Bayesian evidence. We compute the Bayesian evidence under the assumption that the data either contain a coherent gravitational-wave signal, noise, or a glitch (Z^S, Z^N, Z^G, defined in Appendix A). However, instead of computing true Bayesian odds, we use the evidences as a ranking statistic. We form a bootstrapped distribution of the evidence for simulated foreground and background events to form a frequentist ranking statistic.

B. Formalism

Introduced by Isi *et al.* [70], the Bayesian Coherence Ratio for a candidate signal in a network of D detectors is given by

$$\rho_{\rm BCR} = \frac{\hat{\pi}^S Z^S}{\prod_{i=1}^{D} [\hat{\pi}^G_i Z^G_i + \hat{\pi}^N_i Z^N_i]} , \tag{1}$$

where $\{\hat{\pi}^S, \hat{\pi}^N_i, \hat{\pi}^G_i\}$ are estimates of the astrophysical prior-odds that the data contain a coherent signal, incoherent noise or an incoherent glitch. We assume each detector has the same glitch and noise prior odds of $\{\hat{\pi}^N, \hat{\pi}^G\}$. In the limit where the estimated prior-odds equal the astrophysical prior-odds, the $\rho_{\rm BCR}$ becomes the optimal Bayesian odds described by Ashton *et al.* [71]. However, as the astrophysical prior-odds are unknown, it is invalid to use the $\rho_{\rm BCR}$ as an odds-ratio to discriminate signals from glitches. Instead, we use the $\rho_{\rm BCR}$ as a ranking statistic to obtain a frequentist significance of a candidate $\rho_{\rm BCR}$-value, $\rho^c_{\rm BCR}$, measured against a background $\rho_{\rm BCR}$ distribution, $\rho^b_{\rm BCR}$.

Since it is impossible to shield ground-based gravitational-wave detectors from gravitational-wave signals, the LVK empirically estimates the background by repeatedly time-shifting strain data by amounts larger than the light-travel time between the two LIGO detectors [74]. We use time-shifted data to generate $\rho^b_{\rm BCR}$. Following this, each candidate's single-event false alarm probability p_1 of being miss-classified as a glitch is given by

$$p_1 = \frac{\text{Count of } \rho^b_{\rm BCR} \leq \rho^c_{\rm BCR}}{\text{Count of } \rho^b_{\rm BCR}} . \tag{2}$$

Moreover, as we have several candidates (N candidates), each with a $\rho^c_{\rm BCR}$, we account for them by calculating a false-alarm probability with trial factors p_N given by

$$p_N = 1 - (1 - p_1)^N . \tag{3}$$

[1] 170222 is a sub-threshold candidate detected by PyCBC ($t_c = 1171814476.97$) with a $p_{\rm S} \sim 0.6$. The prefix of GW is not utilized as this is a candidate event.

TABLE I. Trigger-selection lab-frame parameter space (parameters correspond to signals with durations ≤ 454 ms and $q \geq 0.1$).

	Minimum	Maximum
Component Mass 1 [$M_\odot$]	31.54	491.68
Component Mass 2 [$M_\odot$]	1.32	121.01
Total Mass [$M_\odot$]	56.93	496.72
Chirp Mass [$M_\odot$]	8.00	174.56
Mass Ratio	0.1	0.98

Finally, we can calculate the probability of the candidate signal event occurring from a gravitational-wave, $p_{\rm S}$ with

$$p_{\rm S} = 1 - p_N \ . \tag{4}$$

III. ANALYSIS

We acquire candidate signal triggers (times when the detector's data has a signal-to-noise ratio above a predetermined threshold) for $\rho_{\rm BCR}$ analysis from PyCBC's search in O2 [75–82, 92]. Some of the triggers are associated with gravitational-wave events and candidates while others are glitches. We also acquire background and simulated triggers from PyCBC's O2 search to calculate $\rho^b_{\rm BCR}$ and estimate values for $\{\hat{\pi}^S, \hat{\pi}^G\}$ (see Appendix B for details on the estimation process). The triggers are divided into two week time-frames because the detector's sensitivity does not stay constant throughout the eight-month-long observing period [80].

For our study, we filter PyCBC triggers to include only those in the parameter ranges presented in Table I. This region focuses our analysis on binary black hole mergers with lab-frame total masses above $\gtrsim 55 M_\odot$, corresponding to binary systems with signal durations < 454 ms and $q \geq 0.1$. The filtering process leaves us with 60,996 background, 5,146 simulated, and 25 candidate signal triggers. We additionally include events and candidate events reported by GWTC-1 and the IAS group in our list of candidate signal triggers. A plot of the lab-fame component mass space constrained by our search space is presented in Fig. 1.

To evaluate $\{Z^S, Z^G_i, Z^N_i\}$ and calculate the $\rho_{\rm BCR}$ Eq. 1 for triggers, we carry out Bayesian inference with `bilby` [93, 94], employing `dynesty` [95] as our nested sampler. Nested sampling, an algorithm introduced by Skilling [96, 97], provides an estimate of the Bayesian evidence and is often utilized for parameter estimation within the LIGO collaboration [93, 98, 99].

We use a likelihood that marginalizes over coalescence time, the phase at coalescence, and luminosity distance (Eq. 80 from Thrane and Talbot [100]). We use identical parameter estimation priors for the glitch and signal models. We restrict the spin priors to aligned spins to reduce the number of parameters we sample. We define our mass priors to be uniform in chirp mass $\mathcal{M}$ and mass ratio q to avoid sampling issues that arise from sampling in thin regions of the component mass parameter space [101]. As a post-processing step, we convert posterior samples calculated with uniform $\{\mathcal{M}, q\}$ priors to uniform component mass priors by re-sampling the posterior samples using the Jacobian given in Eq. 21 of Veitch *et al.* [102]. The complete list of the priors is in Table II.

TABLE II. Prior settings for the lab-frame parameters used during our parameter estimation. The definitions of the parameters are documented in Romero-Shaw *et al.* [101] Table E1. The trigger time t_c is obtained from the data products of PyCBC's O2 search.

Parameter	Shape	Limits
$\mathcal{M}/M_\odot$	Uniform	7–180
q	Uniform	0.1–1
$M/M_\odot$	Constraint	50–500
$d_{\rm L}$/Mpc	Comoving	100–5000
χ_1, χ_2	Uniform	-1–1
θ_{JN}	Sinusoidal	0–π
ψ	Uniform	0–π
ϕ	Uniform	0–2π
ra	Uniform	0–2π
dec	Cosine	0–2π
t_c/s	Uniform	$t_c \pm 0.1$

The waveform template we utilize is `IMRPhenomPv2`, a phenomenological waveform template constructed in the frequency domain that models the in-spiral, merger, and ring-down (IMR) of a compact binary coalescence [103]. Although there exist gravitational-wave templates such as `IMRPhenomXPHM` [104], `NRSur7dq4` [105] and `SEOBNRv4PHM` [106] which incorporate more physics, such as information on higher-order modes, we use `IMRPhenomPv2` as it is computationally inexpensive compared to others.

To generate the PSD, we take 31 neighboring off-source non-overlapping 4-second segments of time-series data before the analysis data segment d_i. A Tukey window with a 0.2-second roll-off is applied to each data segment to suppress spectral leakage. After this, we fast-Fourier transform and median-average the segments to create a PSD [107]. Like other PSD estimation methods, this method adds statistical uncertainties to the PSD [108–110]. To marginalize over the statistical uncertainty, we use the median-likelihood presented by Talbot and Thrane [108] as a post-processing step. We find that this post-processing step improves the search efficiency by 49.26% the details of this calculation are in the Appendix C.

The data we use are the publicly accessible O2 strain data from the Hanford and Livingston detectors, recorded while the detectors are in "Science Mode". We obtain the data from the gravitational-wave Open Science Center [111] using `GWpy` [112].

Finally, with the $\rho^c_{\rm BCR}$ and $\rho^b_{\rm BCR}$ for each time-frame of triggers, we calculate the candidate signal's $p_{\rm S}$.

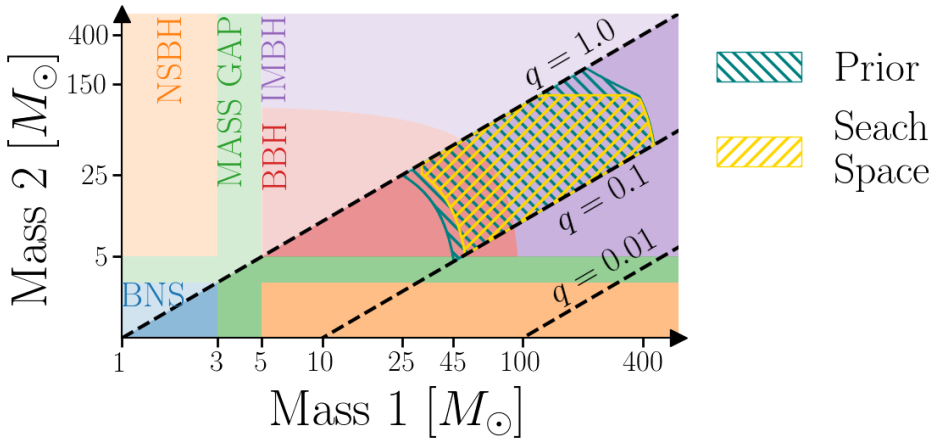

FIG. 1. Lab-frame component-mass boundaries for our search space and parameter estimation prior. Our search is constrained to the parameter space enclosed by the gold-colored hatches, while our prior is constrained to the slightly larger parameter space enclosed by the teal-colored hatches. The purple region labeled "IMBH" is the parameter space where merger remnants may be IMBHs.

IV. RESULTS

We analyze the O2 candidates with $M_T^{\rm lab} > 55\ M_\odot$ and report candidates with $p_{\rm S} \geq 0.2$ in Table III. The $\hat{\pi}^S$ and $\hat{\pi}^G$ values utilized for each time-frame are reported in Appendix D. By imposing a $p_{\rm S}$ threshold of 0.5, we present 13 candidate gravitational wave events.

Various search pipeline $p_{\rm astro}$ are not mathematically equivalent [113]. Moreover, $p_{\rm astro}$ is not equivalent to $p_{\rm S}$. However, by comparing candidates' various $p_{\rm astro}$ values with $p_{\rm S}$, we can compare how significant each pipeline deems the candidate. For comparison, in Table III we report $p_{\rm astro}$ values from GWTC-1 [74], PyCBC OGC-2 [84], PyCBC OGC-3 [84], PyCBC 'single-search' [83], IAS [86, 87], and Pratten and Vecchio [73]'s analyses.

A. GWTC-1 Events

All the confirmed gravitational-wave events from binary black hole mergers reported in GWTC-1 and within our prior space (specifically GW170104, GW170608, GW170729, GW170809, and GW170814) have $p_{\rm S} > 0.9$, indicating a high probability of an astrophysical signal.

In addition to the above confirmed gravitational-wave events from GWTC-1, we have also analyzed several candidate events from GWTC-1, most of which have low $p_{\rm S}$. For example, consider the candidate event 170412 ($t_c = 1176047817$), assigned a $p_{\rm astro}$ of 0.06 by GstLAL and has a $p_{\rm S}$ of 0.01. This candidate was reported to be excess power caused due to noise appearing non-stationary between $60 - 200$ Hz [74]. This candidate demonstrates that $p_{\rm S}$ may be utilized to eliminate candidates originating from terrestrial noise sources.

B. IAS Events

Our analysis of the IAS events and candidates with $M_T^{\rm lab} \gtrsim 55\ M_\odot$ in O2 has resulted in one event with disfavored $p_{\rm S} < 0.5$ (GW170425), and five events and two candidates with $p_{\rm S} \geq 0.5$ (GW170121, GW170304, 170302, GWC170402, GW170403, GW170727, GW170817A). From this list, four events (GW170121, GW170304, GW170727, GW170817A) have $p_{\rm S} > 0.8$ and $p_{\rm astro} > 0.9$ reported from other pipelines, making them viable gravitational-wave event candidates.

GWC170402, detected by Zackay *et al.* [87], is reported to originate from a binary with non-zero eccentricity [87]. As we used a non-eccentric waveform during analysis, we may be under estimating this event's significance at $p_{\rm S} \leq 0.6$. Finally, GW170425 which has $p_{\rm S} < 0.25$ also has low $p_{\rm astro}$ reported in OGC-2 and OGC-3 [84, 114], suggesting that GW170425 may have been false alarm.

C. New Candidate Events

Although no IMBH detections are made with the $\rho_{\rm BCR}$, a marginal stellar mass black hole merger candidate 170222 has been discovered with a $p_{\rm S} \sim 0.6$. This candidate has a SNR ~ 7.7, low spin magnitudes, and source-frame component masses of $(47.16^{+8.00}_{-5.77}, 35.50^{+5.79}_{-6.35})M_\odot$ (90% credible intervals), making it one of the heavier black-hole mergers from O2 and GWTC-1. This candidate may be of interest as one component black hole may lie in the pair-instability mass gap $(55^{+10}_{-10} - 148^{+13}_{-12})M_\odot$ [115, 116]. More details on the candidate are presented in Appendix E. The remaining coherent trigger candidates all have $p_{\rm S} < 0.5$, making them unlikely to originate from astrophysical sources.

TABLE III. $p_{\rm S}$ table for gravitational wave events and candidates in our search space with $p_{\rm S} > 0.2$, calculated using Hanford and Livingston observatory data. Displayed for comparison are significances of events taken from: GstLAL $p^{\rm GstLAL}_{\rm astro}$ [74], PyCBC $p^{\rm pyCBC}_{\rm astro}$ [74], IAS $p^{\rm IAS}_{\rm astro}$ [86, 87], $P(S|{\rm d})$ [73], PyCBC 'single-search' $p^{\rm S}_{\rm astro}$ [83], PyCBC OGC-2 $p^{\rm OGC2}_{\rm astro}$ [84] and PyCBC OGC-3 $p^{\rm OGC3}_{\rm astro}$ [84]. The t_c column contains the 'GPS' coalescence-times of the gravitational wave events. The catalog column displays the first catalog reporting the event on each row (the catalogs labeled IAS-1 and IAS-2 correspond to the candidates published in Venumadhav *et al.* [86] and Zackay *et al.* [87]).

Event	Catalog	$p_{\rm S}$	$p^{\rm pyCBC}_{\rm astro}$	$p^{\rm GstLAL}_{\rm astro}$	$p^{\rm IAS}_{\rm astro}$	$P(S\|{\rm d})$	$p^{\rm S}_{\rm astro}$	$p^{\rm OGC2}_{\rm astro}$	$p^{\rm OGC3}_{\rm astro}$	t_c
GW170104	GWTC-1	0.97	1.00	1.00		1.00		1.00		1167559936.60
GW170121	IAS-1	0.83			1.00	0.53		1.00	1.00	1169069154.57
170209	-	0.32								1170659643.47
170222	-	0.58								1171814476.97
170302	IAS-1	0.78			0.45					1172487817.48
GW170304	IAS-1	0.94			0.99	0.03		0.70	0.70	1172680691.36
GWC170402	IAS-2	0.60			0.68	0.00				1175205128.57
GW170403	IAS-1	0.54			0.56	0.27		0.03	0.71	1175295989.22
170421	-	0.27								1176789158.14
GW170425	IAS-1	0.22			0.77	0.74		0.21	0.41	1177134832.18
GW170608	GWTC-1	0.99	1.00	0.92		1.00				1180922494.50
GW170727	IAS-1	0.98			0.98	0.66		0.99	1.00	1185152688.02
GW170729	GWTC-1	0.98	0.52	0.98		1.00		1.00	0.99	1185389807.30
GW170809	GWTC-1	0.99	1.00	0.99		1.00		1.00	1.00	1186302519.75
GW170814	GWTC-1	1.00	1.00	1.00		1.00		1.00	1.00	1186741861.53
GW170817A	IAS-2	0.92			0.86	0.02				1186974184.72

V. CONCLUSION

In this paper, we demonstrate that the Bayesian Coherence Odds-Ratio $\rho_{\rm BCR}$ [70] can be used as a ranking statistic to provide a measure of significance for gravitational-wave signals originating from CBCs with lab-frame total masses between 55 $M_\odot$ and 400 $M_\odot$, a range that includes IMBHs. To compute the $\rho_{\rm BCR}$ for candidates, we utilize Bayesian inference to calculate the probability of data under various hypotheses (the hypotheses that the data contains a coherent signal, just noise, or an incoherent glitch). This Bayesian ranking method takes a step towards building a unified Bayesian framework that provides a measure of significance for candidates and estimates their parameters, utilizing the same level of physical information incorporated during detected parameter estimation studies.

In our study, we analyze O2 binary-black hole events and candidates with $M_T^{\rm lab} > 55\ M_\odot$ reported by the PyCBC search [84], the IAS-team [86, 87] and those reported in GWTC-1 [74]. Using a $p_{\rm S}$ threshold of 0.5, we find that the GWTC-1 events have high probabilities of originating from an astrophysical source. We also find that some of the GWTC-1 marginal triggers that have corroborated terrestrial sources (for example, candidate 170412) have low $p_{\rm S}$, indicating this method's ability to discriminate between terrestrial artifacts and astrophysical signals. Our analysis of the IAS events demonstrates that GW170121, GW170304, GW170727, and GW170817A are likely to originate from astrophysical sources ($p_{\rm S} \geq 0.8$), while GW170425 is not ($p_{\rm S} < 0.25$). Finally, we report a new marginal binary-black hole merger candidate, 170222.

With the rapid rate of development in gravitational-wave Bayesian inference, we anticipate the ability to analyze longer-duration signals, utilize more advanced signal and glitch models, and incorporate data from the entire detector network. In a similar vein, with the accumulation of more gravitational wave events, future $\rho_{\rm BCR}$ work may utilize astrophysically informed priors during Bayesian inference and more accurate prior odds for each detector.

ACKNOWLEDGMENTS

The authors gratefully thank the PyCBC team for providing the gravitational-wave foreground, background, and simulated triggers from PyCBC's search of O2's data. We also warmly thank Ian Harry and Thomas Dent for answering questions about the PyCBC search's data products.

We gratefully acknowledge the computational resources provided by the LIGO Laboratory—Caltech Computing Cluster and supported by NSF grants PHY-0757058 and PHY-0823459, and thank Stuart Anderson for his assistance in resource scheduling.

All analyses (inclusive of test and failed analyses) performed for this study used 1.3M core-hours, amounting to a carbon footprint of ~ 167 t of CO_2 (using the U.S. average electricity source emissions of 0.429 kg/kWh [117] and 0.3 kWh for each CPU).

This work is supported by the Australian Research Council (ARC) Centre of Excellence CE170100004. This material is based upon work supported by NSF's LIGO Laboratory, a major facility fully funded by the National Science Foundation. This research has used data, software, and web tools obtained from the Gravitational Wave Open Science Center (https://www.gw-openscience.org), a service of LIGO Laboratory, the LIGO Scientific Collaboration and the Virgo Collaboration. LIGO Laboratory and Advanced LIGO are funded by the United States National Science Foundation (NSF) as well as the Science and Technology Facilities Council (STFC) of the United Kingdom, the Max-Planck-Society (MPS), and the State of Niedersachsen/Germany for support of the construction of Advanced LIGO and construction and operation of the GEO600 detector. Additional support for Advanced LIGO was provided by the Australian Research Council. Virgo is funded, through the European Gravitational Observatory (EGO), by the French Centre National de Recherche Scientifique (CNRS), the Italian Istituto Nazionale di Fisica Nucleare (INFN) and the Dutch Nikhef, with contributions by institutions from Belgium, Germany, Greece, Hungary, Ireland, Japan, Monaco, Poland, Portugal, Spain.

DATA AVAILABILITY STATEMENT

We analyze publicly-available gravitational wave strain data from the LIGO-Virgo-KAGRA collaboration [118]. The trigger times for analysis were provided by the PyCBC team. The derived data generated in this research will be shared on reasonable request to the corresponding author.

Software: `bilby` (version 1.0.0) [93], `bilby-pipe` (version 1.0.0) [94], `dynesty` [95–97], `GWpy` [112], `LALSimulation` [119], `matplotlib` [120], `NumPy` [121], `SciPy` [122], `pandas` [123], `python` [124, 125].

Appendix A: Bayesian Evidence Evaluation

1. Noise Model

We assume that each detector's noise is Gaussian and stationary over the period being analyzed [107]. In practice, we assume that the noise has a mean of zero that the noise variance σ^2 is proportional to the noise power spectral density (PSD) $P(f)$ of the data. Using the $P(f)$, for each frequency-domain data segment d_i in each of the i detectors in a network of D detectors, we can write

$$Z_i^N = \mathcal{N}(d_i|\mu = 0, \sigma^2 = P(f)), \tag{A1}$$

where $\mathcal{N}$ is a normal distribution.

2. Coherent Signal Model

We model coherent signals using a binary black hole waveform template $\mu(\vec{\theta})$, where the vector $\vec{\theta}$ contains a point in the 11-dimensional space describing aligned-spin binary-black hole mergers. For the signal to be coherent, $\vec{\theta}$ must be consistent in each 4-second data segment d_i for a network of D detectors. Hence, the coherent signal evidence is calculated as

$$Z^S = \int_{\vec{\theta}} \prod_{i=1}^{D} \left[\mathcal{L}(d_i|\mu(\vec{\theta}))\right] \pi(\vec{\theta}|\mathcal{H}_S)\, \mathrm{d}\vec{\theta}\,, \tag{A2}$$

where $\pi(\vec{\theta}|\mathcal{H}_S)$ is the prior for the parameters in the coherent signal hypothesis $\mathcal{H}_S$, and $\mathcal{L}(d_i|\mu(\vec{\theta}))$ is the likelihood for the coherent signal hypothesis that depends on the gravitational-wave template $\mu(\vec{\theta})$ and its parameters $\vec{\theta}$.

3. Incoherent Glitch Model

Finally, as glitches are challenging to model and poorly understood, we follow Veitch and Vecchio [68] and utilize a surrogate model for glitches. The glitches are modeled using gravitational-wave templates $\mu(\vec{\theta})$ with uncorrelated parameters amongst the different detectors such that $\vec{\theta}_i \neq \vec{\theta}_j$ for two detectors i and j [68]. Modeling glitches with $\mu(\vec{\theta})$ captures the worst-case scenario: when glitches are identical to gravitational-wave signals (excluding coherent signals). Thus, we can write Z_i^G as

$$Z_i^G = \int_{\vec{\theta}} \mathcal{L}(d_i|\mu(\vec{\theta}))\ \pi(\vec{\theta}|\mathcal{H}_G)\ \mathrm{d}\vec{\theta}\,, \tag{A3}$$

where $\pi(\theta|\mathcal{H}_G)$ is the prior for the parameters in the incoherent glitch hypothesis $\mathcal{H}_G$.

Appendix B: Tuning the prior-odds

After calculating the ρ_{BCR} for a set of background triggers and simulated triggers from as stretch of detector-data (a data chunk), we can compute probability distributions for the background and simulated triggers,

$p_b(\rho_{\rm BCR})$ and $p_s(\rho_{\rm BCR})$. We expect the background trigger and simulated signal $\rho_{\rm BCR}$ values to favor the incoherent glitch and the coherent signal hypothesis, respectively. Ideally, these distributions representing two unique populations should be distinctly separate and have no overlap in their $\rho_{\rm BCR}$ values. The prior odds parameters $\hat{\pi}^S$ and $\hat{\pi}^G$ from Eq. 1 help separate the two distributions. Altering $\hat{\pi}^S$ translates the $\rho_{\rm BCR}$ probability distributions while adjusting $\hat{\pi}^G$ spreads the distributions (refer to Appendix A of Isi *et al.* [70]). Although Bayesian hyper-parameter estimation can determine the optimal values for $\hat{\pi}^S$ and $\hat{\pi}^G$, an easier approach is to adjust the parameters for each data chunk's $\rho_{\rm BCR}$ distribution. In this study, we tune $\hat{\pi}^S$ and $\hat{\pi}^G$ to maximally separate the $\rho_{\rm BCR}$ distributions for the background and simulated triggers.

To calculate the separation between $p_b(\rho_{\rm BCR})$ and $p_s(\rho_{\rm BCR})$, we use the Kullback–Leibler divergence (KL divergence) D_{KL}, given by

$$D_{KL}(p_b|p_s) = \sum_{x\in\rho_{\rm BCR}} p_b(x)\log\left(\frac{p_b(x)}{p_a(x)}\right) . \qquad \text{(B1)}$$

The $D_{K.L.} = 0$ when the distributions are identical and increases as the asymmetry between the distributions increases.

We limit our search for the maximum KL-divergence in the $\hat{\pi}^S$ and $\hat{\pi}^G$ ranges of $[10^{-10}, 10^0]$. We set our values for $\hat{\pi}^S$ and $\hat{\pi}^G$ to those which provide the highest KL-divergence and calculate the $\rho_{\rm BCR}$ for candidate events present in this data chunk. Note that we conduct the analysis in data chunks of a few days rather than an entire data set of a few months as the background may be different at different points of the entire data set.

Appendix C: Marginalizing over PSD statistical uncertainties

To generate the results presented in Table III, we applied a post-processing step to marginalize the uncertainty in the PSD. In Fig. 2, we demonstrate the impact of the post-processing step. Marginalizing over uncertainty in the PSD yields an improvement in the separation of the noise and signal distributions (left plot). Quantitatively, at a threshold ${\rho_{\rm BCR}}^T = 0$ the post-processing step results in a reduction in the number of background $\rho_{\rm BCR} > {\rho_{\rm BCR}}^T$ from 60.7% to 25.28% in the August 13 - 21, 2017 time-frame of data. For the entirety of O2, PSD marginalization resulted in a 49.26% improvement in search efficiency.

Appendix D: Tuned prior odds

O2 lasted several months, over which the detector's sensitivity varied. Hence, a part of our analysis entailed tuning the prior odds for obtaining a signal and a glitch, $\hat{\pi}^S$ and $\hat{\pi}^G$, as described in Section II. Table IV presents the signal and glitch prior odds utilized for each time-frame of O2 data.

TABLE IV. The prior odds used for each time-frame of data from O2. Each time frame commences at the start date and concludes at the following time-frame's start date.

Start Date	$\hat{\pi}^S$	$\hat{\pi}^G$
2016-12-23	1.00E+00	6.25E-01
2017-01-22	1.00E+00	2.33E-02
2017-02-03	1.00E-10	2.44E-01
2017-02-12	1.76E-08	5.96E-02
2017-02-20	6.55E-10	2.22E-03
2017-02-28	1.00E-10	5.96E-02
2017-03-10	2.56E-10	3.91E-01
2017-03-18	1.60E-10	1.00E+00
2017-03-27	1.10E-08	5.96E-02
2017-04-04	3.73E-02	2.33E-02
2017-04-14	1.05E-09	2.44E-01
2017-04-23	2.68E-09	1.46E-02
2017-05-08	1.00E+00	2.44E-01
2017-06-18	6.55E-10	3.39E-04
2017-06-30	2.02E-05	5.69E-03
2017-07-15	1.05E-09	9.54E-02
2017-07-27	1.00E+00	2.12E-04
2017-08-05	2.12E-04	3.73E-02
2017-08-13	2.68E-09	8.69E-04

Tuning the prior odds can dramatically affect the $p_{\rm S}$. For example, consider Table V, which reports tuned $p_{\rm S}$ and un-tuned $p'_{\rm S}$ (where $\hat{\pi}^S = 1$ and $\hat{\pi}^G = 1$) for various events and candidates. By tuning the prior odds, the $p_{\rm S}$ for some IAS events (for example, GW170403 and GW170817A) can change by more than 0.5, resulting in the promotion/demotion of a candidate's significance.

Appendix E: A closer look at 170222

PyCBC found the candidate 170222 with $\mathcal{M}_c = 49.46$ and $q = 0.68$, values contained inside the 90% credible intervals of our posterior probability distributions for 170222. Some of the posteriors produced as a by-product of our $\rho_{\rm BCR}$ calculation can be viewed in Fig. 3.

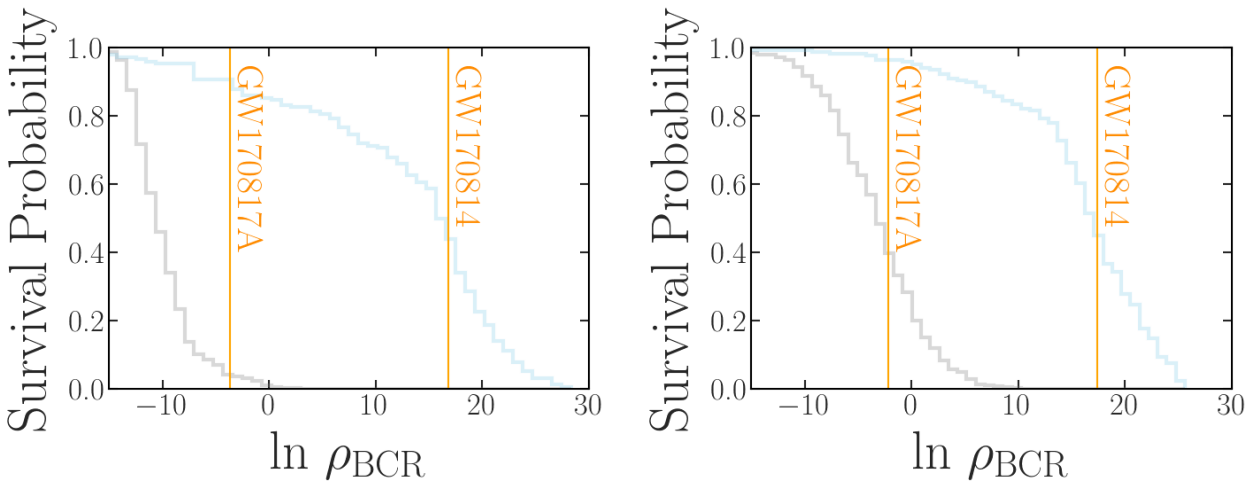

FIG. 2. Histograms represent the survival function (1-CDF) from our selection of background triggers (gray) and simulated signals (blue) triggers obtained from PyCBC's search of data from August 13 - 21, 2017. Vertical lines mark the ln $\rho_{\rm BCR}$ of IAS's GW170817A and GWTC-1's GW170814. Left: Survival functions using the post-processing step to marginalize over PSD statistical uncertainties. Right: Survival functions without the post-processing step. Without the post-processing step, there is a greater overlap between the background (gray) and foreground (blue) survival functions.

TABLE V. Table of $p_{\rm S}$ using "tuned" prior odds and $p_{\rm S}$ using uninformed prior odds of $\hat{\pi}^S = 1$ and $\hat{\pi}^G = 1$ (represented by $p'_{\rm S}$). Details of other columns provided in Table III.

Event	Catalog	$p_{\rm S}$	$p'_{\rm S}$	t_c
GW170104	GWTC-1	0.97	0.95	1167559936.60
GW170121	IAS-1	0.83	0.68	1169069154.57
170209	-	0.32	0.00	1170659643.47
170222	-	0.58	0.50	1171814476.97
170302	IAS-1	0.78	0.54	1172487817.48
GW170304	IAS-1	0.94	0.80	1172680691.36
GWC170402	IAS-2	0.60	0.00	1175205128.57
GW170403	IAS-1	0.54	0.90	1175295989.22
170421	-	0.27	0.21	1176789158.14
GW170425	IAS-1	0.22	0.16	1177134832.18
GW170608	GWTC-1	0.99	0.99	1180922494.50
GW170727	IAS-1	0.98	0.99	1185152688.02
GW170729	GWTC-1	0.98	0.95	1185389807.30
GW170809	GWTC-1	0.99	0.99	1186302519.75
GW170814	GWTC-1	1.00	1.00	1186741861.53
GW170817A	IAS-2	0.92	0.30	1186974184.72

[1] B. M. Peterson, Measuring the Masses of Supermassive Black Holes, Space Sci. Rev. **183**, 253 (2014).
[2] R. Schödel, T. Ott, R. Genzel, R. Hofmann, and et al., A star in a 15.2-year orbit around the supermassive black hole at the centre of the Milky Way, Nature **419**, 694 (2002), arXiv:astro-ph/0210426 [astro-ph].
[3] B. Kızıltan, H. Baumgardt, and A. Loeb, An intermediate-mass black hole in the centre of the glob-

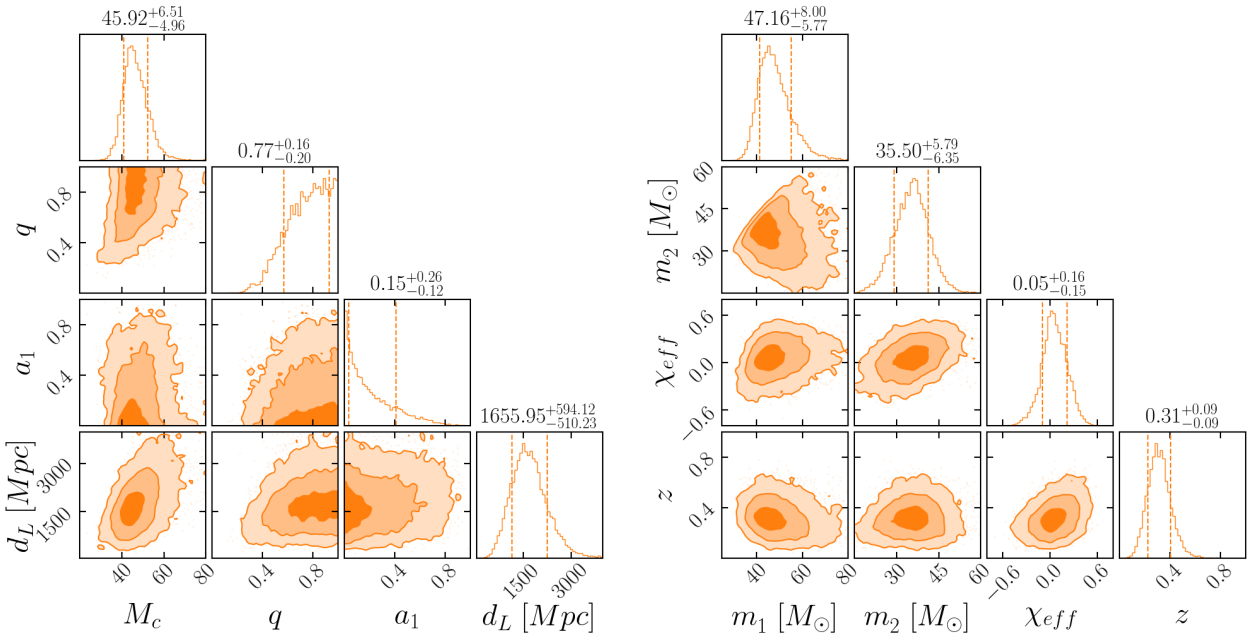

FIG. 3. Posterior distributions for 8 parameters of 170222. Left: Posterior probability distributions for 4 of the 12 search parameters. Right: Posterior probability distributions for 4 derived parameters.

ular cluster 47 Tucanae, Nature **542**, 203 (2017), arXiv:1702.02149 [astro-ph.GA].

[4] A. W. Graham and N. Scott, The M $_{BH}$-L $_{spheroid}$ Relation at High and Low Masses, the Quadratic Growth of Black Holes, and Intermediate-mass Black Hole Candidates, ApJ **764**, 151 (2013), arXiv:1211.3199 [astro-ph.CO].

[5] T. Wevers, S. van Velzen, P. G. Jonker, N. C. Stone, T. Hung, F. Onori, S. Gezari, and N. Blagorodnova, Black hole masses of tidal disruption event host galaxies, MNRAS **471**, 1694 (2017), arXiv:1706.08965 [astro-ph.GA].

[6] J. E. Greene and L. C. Ho, Active Galactic Nuclei with Candidate Intermediate-Mass Black Holes, ApJ **610**, 722 (2004), arXiv:astro-ph/0404110 [astro-ph].

[7] D. Lin, J. Strader, A. J. Romanowsky, J. A. Irwin, O. Godet, D. Barret, N. A. Webb, J. Homan, and R. A. Remillard, Multiwavelength Follow-up of the Hyperluminous Intermediate-mass Black Hole Candidate 3XMM J215022.4-055108, ApJ **892**, L25 (2020), arXiv:2002.04618 [astro-ph.HE].

[8] J. Paynter, R. Webster, and E. Thrane, Evidence for an intermediate-mass black hole from a gravitationally lensed gamma-ray burst, Nature Astronomy 10.1038/s41550-021-01307-1 (2021).

[9] J. E. Greene, J. Strader, and L. C. Ho, Intermediate-Mass Black Holes, ARA&A **58**, 257 (2020), 2021 review on IMBH, arXiv:1911.09678 [astro-ph.GA].

[10] F. Koliopanos, Intermediate Mass Black Holes: A Review, in *XII Multifrequency Behaviour of High Energy Cosmic Sources Workshop (MULTIF2017)* (2017) p. 51, arXiv:1801.01095 [astro-ph.GA].

[11] M. Mezcua, Observational evidence for intermediate-mass black holes, International Journal of Modern Physics D **26**, 1730021 (2017), arXiv:1705.09667 [astro-ph.GA].

[12] A. Ridolfi, P. C. C. Freire, P. Torne, C. O. Heinke, and et al., Long-term observations of the pulsars in 47 Tucanae - I. A study of four elusive binary systems, MNRAS **462**, 2918 (2016), arXiv:1607.07248 [astro-ph.HE].

[13] P. C. C. Freire, A. Ridolfi, M. Kramer, C. Jordan, and et al., Long-term observations of the pulsars in 47 Tucanae - II. Proper motions, accelerations and jerks, MNRAS **471**, 857 (2017), arXiv:1706.04908 [astro-ph.HE].

[14] G. L. Israel, A. Papitto, P. Esposito, L. Stella, and et al., Discovery of a 0.42-s pulsar in the ultraluminous X-ray source NGC 7793 P13, MNRAS **466**, L48 (2017), arXiv:1609.06538 [astro-ph.HE].

[15] G. A. Rodríguez Castillo, G. L. Israel, A. Belfiore, F. Bernardini, and et al., Discovery of a 2.8 s Pulsar in a 2 Day Orbit High-mass X-Ray Binary Powering the Ultraluminous X-Ray Source ULX-7 in M51, ApJ **895**, 60 (2020), arXiv:1906.04791 [astro-ph.HE].

[16] B. L. Webster and P. Murdin, Cygnus X-1-a Spectroscopic Binary with a Heavy Companion ?, Nature **235**, 37 (1972).

[17] B. Balick and R. L. Brown, Intense sub-arcsecond structure in the galactic center., ApJ **194**, 265 (1974).

[18] A. M. Ghez, B. L. Klein, M. Morris, and E. E. Becklin, High Proper-Motion Stars in the Vicinity of Sagittarius A*: Evidence for a Supermassive Black Hole at the Center of Our Galaxy, ApJ **509**, 678 (1998), arXiv:astro-ph/9807210 [astro-ph].

[19] R. Genzel, F. Eisenhauer, and S. Gillessen, The Galactic Center massive black hole and nuclear star cluster, Reviews of Modern Physics **82**, 3121 (2010), arXiv:1006.0064 [astro-ph.GA].

[20] B. P. Abbott, R. Abbott, T. D. Abbott, S. Abraham, and et al., GWTC-1: A Gravitational-Wave Transient Catalog of Compact Binary Mergers Observed by LIGO

and Virgo during the First and Second Observing Runs, Physical Review X **9**, 031040 (2019), arXiv:1811.12907 [astro-ph.HE].

[21] Event Horizon Telescope Collaboration, K. Akiyama, A. Alberdi, W. Alef, and et al., First M87 Event Horizon Telescope Results. I. The Shadow of the Supermassive Black Hole, ApJ **875**, L1 (2019), arXiv:1906.11238 [astro-ph.GA].

[22] R. Abbott, T. D. Abbott, S. Abraham, F. Acernese, and et al., GWTC-2: Compact Binary Coalescences Observed by LIGO and Virgo During the First Half of the Third Observing Run, arXiv e-prints , arXiv:2010.14527 (2020), arXiv:2010.14527 [gr-qc].

[23] H. Tagawa, B. Kocsis, Z. Haiman, I. Bartos, K. Omukai, and J. Samsing, Mass-gap Mergers in Active Galactic Nuclei, ApJ **908**, 194 (2021), arXiv:2012.00011 [astro-ph.HE].

[24] Y.-P. Li, A. M. Dempsey, S. Li, H. Li, and J. Li, Orbital evolution of binary black holes in active galactic nucleus disks: a disk channel for binary black hole mergers?, arXiv e-prints , arXiv:2101.09406 (2021), arXiv:2101.09406 [astro-ph.HE].

[25] J. Samsing, I. Bartos, D. J. D'Orazio, Z. Haiman, B. Kocsis, N. W. C. Leigh, B. Liu, M. E. Pessah, and H. Tagawa, Active Galactic Nuclei as Factories for Eccentric Black Hole Mergers, arXiv e-prints , arXiv:2010.09765 (2020), arXiv:2010.09765 [astro-ph.HE].

[26] H. Tagawa, Z. Haiman, and B. Kocsis, Formation and Evolution of Compact-object Binaries in AGN Disks, ApJ **898**, 25 (2020), arXiv:1912.08218 [astro-ph.GA].

[27] W. Ishibashi and M. Gröbner, Evolution of binary black holes in AGN accretion discs: Disc-binary interaction and gravitational wave emission, A&A **639**, A108 (2020), arXiv:2006.07407 [astro-ph.GA].

[28] M. Gröbner, W. Ishibashi, S. Tiwari, M. Haney, and P. Jetzer, Binary black hole mergers in AGN accretion discs: gravitational wave rate density estimates, A&A **638**, A119 (2020), arXiv:2005.03571 [astro-ph.GA].

[29] Y. Yang, I. Bartos, V. Gayathri, K. E. S. Ford, and et al., Hierarchical Black Hole Mergers in Active Galactic Nuclei, Phys. Rev. Lett. **123**, 181101 (2019), arXiv:1906.09281 [astro-ph.HE].

[30] B. McKernan, K. E. S. Ford, I. Bartos, M. J. Graham, W. Lyra, S. Marka, Z. Marka, N. P. Ross, D. Stern, and Y. Yang, Ram-pressure Stripping of a Kicked Hill Sphere: Prompt Electromagnetic Emission from the Merger of Stellar Mass Black Holes in an AGN Accretion Disk, ApJ **884**, L50 (2019), arXiv:1907.03746 [astro-ph.HE].

[31] Y. Yang, I. Bartos, Z. Haiman, B. Kocsis, Z. Márka, N. C. Stone, and S. Márka, AGN Disks Harden the Mass Distribution of Stellar-mass Binary Black Hole Mergers, ApJ **876**, 122 (2019), arXiv:1903.01405 [astro-ph.HE].

[32] B. McKernan, K. E. S. Ford, J. Bellovary, N. W. C. Leigh, and et al., Constraining Stellar-mass Black Hole Mergers in AGN Disks Detectable with LIGO, ApJ **866**, 66 (2018), arXiv:1702.07818 [astro-ph.HE].

[33] J. M. Bellovary, M.-M. Mac Low, B. McKernan, and K. E. S. Ford, Migration Traps in Disks around Supermassive Black Holes, ApJ **819**, L17 (2016), arXiv:1511.00005 [astro-ph.GA].

[34] B. McKernan, K. E. S. Ford, B. Kocsis, W. Lyra, and L. M. Winter, Intermediate-mass black holes in AGN discs - II. Model predictions and observational constraints, MNRAS **441**, 900 (2014), arXiv:1403.6433 [astro-ph.GA].

[35] B. McKernan, K. E. S. Ford, W. Lyra, and H. B. Perets, Intermediate mass black holes in AGN discs - I. Production and growth, MNRAS **425**, 460 (2012), arXiv:1206.2309 [astro-ph.GA].

[36] S. Banerjee, Stellar-mass black holes in young massive and open stellar clusters - V. comparisons with LIGO-Virgo merger rate densities, MNRAS **503**, 3371 (2021), arXiv:2011.07000 [astro-ph.HE].

[37] M. Zevin, S. S. Bavera, C. P. L. Berry, V. Kalogera, T. Fragos, P. Marchant, C. L. Rodriguez, F. Antonini, D. E. Holz, and C. Pankow, One Channel to Rule Them All? Constraining the Origins of Binary Black Holes Using Multiple Formation Pathways, ApJ **910**, 152 (2021), arXiv:2011.10057 [astro-ph.HE].

[38] M. Mapelli, M. Dall'Amico, Y. Bouffanais, N. Giacobbo, and et al., Hierarchical black hole mergers in young, globular and nuclear star clusters: the effect of metallicity, spin and cluster properties, arXiv e-prints , arXiv:2103.05016 (2021), arXiv:2103.05016 [astro-ph.HE].

[39] N. C. Weatherford, G. Fragione, K. Kremer, S. Chatterjee, C. S. Ye, C. L. Rodriguez, and F. A. Rasio, Black Hole Mergers from Star Clusters with Top-heavy Initial Mass Functions, ApJ **907**, L25 (2021), arXiv:2101.02217 [astro-ph.GA].

[40] Y. Bouffanais, M. Mapelli, F. Santoliquido, N. Giacobbo, U. N. Di Carlo, S. Rastello, M. C. Artale, and G. Iorio, New insights on binary black hole formation channels after GWTC-2: young star clusters versus isolated binaries, arXiv e-prints , arXiv:2102.12495 (2021), arXiv:2102.12495 [astro-ph.HE].

[41] A. Ballone, S. Torniamenti, M. Mapelli, U. N. Di Carlo, M. Spera, S. Rastello, N. Gaspari, and G. Iorio, From hydrodynamics to N-body simulations of star clusters: mergers and rotation, MNRAS **501**, 2920 (2021), arXiv:2012.00767 [astro-ph.GA].

[42] J. Kumamoto, M. S. Fujii, A. A. Trani, and A. Tanikawa, Spin distribution of binary black holes formed in open clusters, arXiv e-prints , arXiv:2102.09323 (2021), arXiv:2102.09323 [astro-ph.HE].

[43] S. Banerjee, Stellar-mass black holes in young massive and open stellar clusters - IV. Updated stellar-evolutionary and black hole spin models and comparisons with the LIGO-Virgo O1/O2 merger-event data, MNRAS **500**, 3002 (2021), arXiv:2004.07382 [astro-ph.HE].

[44] M. A. S. Martinez, G. Fragione, K. Kremer, S. Chatterjee, and et al., Black Hole Mergers from Hierarchical Triples in Dense Star Clusters, ApJ **903**, 67 (2020), arXiv:2009.08468 [astro-ph.GA].

[45] I. Romero-Shaw, P. D. Lasky, E. Thrane, and J. Calderón Bustillo, GW190521: Orbital Eccentricity and Signatures of Dynamical Formation in a Binary Black Hole Merger Signal, ApJ **903**, L5 (2020), arXiv:2009.04771 [astro-ph.HE].

[46] O. Anagnostou, M. Trenti, and A. Melatos, Dynamically formed black hole binaries: In-cluster versus ejected mergers, PASA **37**, e044 (2020), arXiv:2009.00178 [astro-ph.HE].

[47] A. Toubiana, L. Sberna, A. Caputo, G. Cusin, and et al., Detectable Environmental Effects in GW190521-like Black-Hole Binaries with LISA, Phys. Rev. Lett. **126**, 101105 (2021), arXiv:2010.06056 [astro-ph.HE].

[48] E. Farrell, J. H. Groh, R. Hirschi, L. Murphy, E. Kaiser, S. Ekström, C. Georgy, and G. Meynet, Is GW190521 the merger of black holes from the first stellar generations?, MNRAS **502**, L40 (2021), arXiv:2009.06585 [astro-ph.SR].

[49] M. Safarzadeh and Z. Haiman, Formation of GW190521 via Gas Accretion onto Population III Stellar Black Hole Remnants Born in High-redshift Minihalos, ApJ **903**, L21 (2020), arXiv:2009.09320 [astro-ph.HE].

[50] B. Liu and V. Bromm, Gravitational waves from Population III binary black holes formed by dynamical capture, MNRAS **495**, 2475 (2020), arXiv:2003.00065 [astro-ph.CO].

[51] K. Inayoshi, R. Hirai, T. Kinugawa, and K. Hotokezaka, Formation pathway of Population III coalescing binary black holes through stable mass transfer, MNRAS **468**, 5020 (2017), arXiv:1701.04823 [astro-ph.HE].

[52] A. Askar, M. B. Davies, and R. P. Church, Formation of supermassive black holes in galactic nuclei - I. Delivering seed intermediate-mass black holes in massive stellar clusters, MNRAS **502**, 2682 (2021), arXiv:2006.04922 [astro-ph.GA].

[53] M. Arca Sedda and A. Mastrobuono-Battisti, Mergers of globular clusters in the Galactic disc: intermediate mass black hole coalescence and implications for gravitational waves detection, arXiv e-prints , arXiv:1906.05864 (2019), arXiv:1906.05864 [astro-ph.GA].

[54] P. Amaro-Seoane, J. R. Gair, M. Freitag, M. C. Miller, I. Mandel, C. J. Cutler, and S. Babak, TOPICAL REVIEW: Intermediate and extreme mass-ratio inspirals—astrophysics, science applications and detection using LISA, Classical and Quantum Gravity **24**, R113 (2007), arXiv:astro-ph/0703495 [astro-ph].

[55] M. A. Gürkan, J. M. Fregeau, and F. A. Rasio, Massive Black Hole Binaries from Collisional Runaways, ApJ **640**, L39 (2006), arXiv:astro-ph/0512642 [astro-ph].

[56] R. Abbott, T. D. Abbott, S. Abraham, F. Acernese, and et al., GW190521: A Binary Black Hole Merger with a Total Mass of 150 $M_\odot$, Phys. Rev. Lett. **125**, 101102 (2020), arXiv:2009.01075 [gr-qc].

[57] B. P. Abbott, R. Abbott, T. D. Abbott, *et al.* (LIGO Scientific Collaboration and Virgo Collaboration), Search for intermediate mass black hole binaries in the first and second observing runs of the Advanced LIGO and Virgo network, arXiv e-prints , arXiv:1906.08000 (2019), arXiv:1906.08000 [gr-qc].

[58] The LIGO Scientific Collaboration, the Virgo Collaboration, and the KAGRA Collaboration, Search for intermediate mass black hole binaries in the third observing run of Advanced LIGO and Advanced Virgo, arXiv e-prints , arXiv:2105.15120 (2021), arXiv:2105.15120 [astro-ph.HE].

[59] K. Chandra, V. Villa-Ortega, T. Dent, C. McIsaac, A. Pai, I. W. Harry, G. S. Cabourn Davies, and K. Soni, An optimized PyCBC search for gravitational waves from intermediate-mass black hole mergers, arXiv e-prints , arXiv:2106.00193 (2021), arXiv:2106.00193 [gr-qc].

[60] LIGO Scientific Collaboration, J. Aasi, B. P. Abbott, R. Abbott, and et al., Advanced LIGO, Classical and Quantum Gravity **32**, 074001 (2015), arXiv:1411.4547 [gr-qc].

[61] D. V. Martynov, E. D. Hall, B. P. Abbott, R. Abbott, and et al., Sensitivity of the Advanced LIGO detectors at the beginning of gravitational wave astronomy, Phys. Rev. D **93**, 112004 (2016), arXiv:1604.00439 [astro-ph.IM].

[62] C. J. Moore, R. H. Cole, and C. P. L. Berry, Gravitational-wave sensitivity curves, Classical and Quantum Gravity **32**, 015014 (2014).

[63] F. Acernese, M. Agathos, K. Agatsuma, D. Aisa, and et al., Advanced Virgo: a second-generation interferometric gravitational wave detector, Classical and Quantum Gravity **32**, 024001 (2015), arXiv:1408.3978 [gr-qc].

[64] X.-Y. Lu, Y.-J. Tan, and C.-G. Shao, Sensitivity functions for space-borne gravitational wave detectors, Phys. Rev. D **100**, 044042 (2019), arXiv:2007.03400 [gr-qc].

[65] A. H. Nitz, Distinguishing short duration noise transients in LIGO data to improve the PyCBC search for gravitational waves from high mass binary black hole mergers, Classical and Quantum Gravity **35**, 035016 (2018), arXiv:1709.08974 [gr-qc].

[66] J. Powell, Parameter estimation and model selection of gravitational wave signals contaminated by transient detector noise glitches, Classical and Quantum Gravity **35**, 155017 (2018), arXiv:1803.11346 [astro-ph.IM].

[67] M. Cabero, A. Lundgren, A. H. Nitz, T. Dent, D. Barker, E. Goetz, J. S. Kissel, L. K. Nuttall, P. Schale, R. Schofield, and D. Davis, Blip glitches in Advanced LIGO data, Classical and Quantum Gravity **36**, 155010 (2019), arXiv:1901.05093 [physics.ins-det].

[68] J. Veitch and A. Vecchio, Bayesian coherent analysis of in-spiral gravitational wave signals with a detector network, Phys. Rev. D **81**, 062003 (2010), arXiv:0911.3820 [astro-ph.CO].

[69] J. B. Kanner, T. B. Littenberg, N. Cornish, M. Millhouse, E. Xhakaj, F. Salemi, M. Drago, G. Vedovato, and S. Klimenko, Leveraging waveform complexity for confident detection of gravitational waves, Physical Review D **93**, 022002 (2016).

[70] M. Isi, R. Smith, S. Vitale, T. J. Massinger, J. Kanner, and A. Vajpeyi, Enhancing confidence in the detection of gravitational waves from compact binaries using signal coherence, Phys. Rev. D **98**, 042007 (2018), arXiv:1803.09783 [gr-qc].

[71] G. Ashton, E. Thrane, and R. J. E. Smith, Gravitational wave detection without boot straps: A Bayesian approach, Phys. Rev. D **100**, 123018 (2019), arXiv:1909.11872 [gr-qc].

[72] G. Ashton and E. Thrane, The astrophysical odds of GW151216, MNRAS 10.1093/mnras/staa2332 (2020), arXiv:2006.05039 [astro-ph.HE].

[73] G. Pratten and A. Vecchio, Assessing gravitational-wave binary black hole candidates with Bayesian odds, arXiv e-prints , arXiv:2008.00509 (2020), arXiv:2008.00509 [gr-qc].

[74] B. P. Abbott, R. Abbott, T. D. Abbott, *et al.* (LIGO Scientific Collaboration and Virgo Collaboration), GWTC-1: A Gravitational-Wave Transient Catalog of Compact Binary Mergers Observed by LIGO and Virgo during the First and Second Observing Runs, Phys. Rev. X **9**, 031040 (2019).

[75] A. Nitz, I. Harry, D. Brown, C. M. Biwer, J. Willis, T. D. Canton, C. Capano, L. Pekowsky, T. Dent, A. R. Williamson, G. S. Davies, S. De, M. Cabero, B. Machenschalk, P. Kumar, S. Reyes, D. Macleod, F. Pannarale, dfinstad, T. Massinger, M. Tápai, L. Singer, S. Khan, S. Fairhurst, S. Kumar, A. Nielsen, shasvath, I. Dorrington, A. Lenon, and H. Gabbard, gwastro/pycbc: PyCBC Release 1.16.4 (2020).

[76] B. Allen, W. G. Anderson, P. R. Brady, D. A. Brown, and J. D. E. Creighton, FINDCHIRP: An algorithm for detection of gravitational waves from inspiraling compact binaries, Phys. Rev. D **85**, 122006 (2012), arXiv:gr-qc/0509116 [gr-qc].

[77] B. Allen, χ^2 time-frequency discriminator for gravitational wave detection, Phys. Rev. D **71**, 062001 (2005), arXiv:gr-qc/0405045 [gr-qc].

[78] A. H. Nitz, T. Dent, T. Dal Canton, S. Fairhurst, and D. A. Brown, Detecting Binary Compact-object Mergers with Gravitational Waves: Understanding and Improving the Sensitivity of the PyCBC Search, ApJ **849**, 118 (2017), arXiv:1705.01513 [gr-qc].

[79] T. Dal Canton, A. H. Nitz, A. P. Lundgren, A. B. Nielsen, D. A. Brown, T. Dent, I. W. Harry, B. Krishnan, A. J. Miller, K. Wette, K. Wiesner, and J. L. Willis, Implementing a search for aligned-spin neutron star-black hole systems with advanced ground based gravitational wave detectors, Phys. Rev. D **90**, 082004 (2014), arXiv:1405.6731 [gr-qc].

[80] S. A. Usman, A. H. Nitz, I. W. Harry, C. M. Biwer, D. A. Brown, M. Cabero, C. D. Capano, T. Dal Canton, T. Dent, S. Fairhurst, M. S. Kehl, D. Keppel, B. Krishnan, A. Lenon, A. Lundgren, A. B. Nielsen, L. P. Pekowsky, H. P. Pfeiffer, P. R. Saulson, M. West, and J. L. Willis, The PyCBC search for gravitational waves from compact binary coalescence, Classical and Quantum Gravity **33**, 215004 (2016), arXiv:1508.02357 [gr-qc].

[81] A. H. Nitz, T. Dal Canton, D. Davis, and S. Reyes, Rapid detection of gravitational waves from compact binary mergers with PyCBC Live, Phys. Rev. D **98**, 024050 (2018), arXiv:1805.11174 [gr-qc].

[82] G. S. Davies, T. Dent, M. Tápai, I. Harry, C. McIsaac, and A. H. Nitz, Extending the PyCBC search for gravitational waves from compact binary mergers to a global network, Phys. Rev. D **102**, 022004 (2020), arXiv:2002.08291 [astro-ph.HE].

[83] A. H. Nitz, T. Dent, G. S. Davies, and I. Harry, A Search for Gravitational Waves from Binary Mergers with a Single Observatory, ApJ **897**, 169 (2020), arXiv:2004.10015 [astro-ph.HE].

[84] A. H. Nitz, T. Dent, G. S. Davies, S. Kumar, C. D. Capano, I. Harry, S. Mozzon, L. Nuttall, A. Lundgren, and M. Tápai, 2-OGC: Open Gravitational-wave Catalog of Binary Mergers from Analysis of Public Advanced LIGO and Virgo Data, ApJ **891**, 123 (2020), arXiv:1910.05331 [astro-ph.HE].

[85] T. Venumadhav, B. Zackay, J. Roulet, L. Dai, and M. Zaldarriaga, New search pipeline for compact binary mergers: Results for binary black holes in the first observing run of Advanced LIGO, Physical Review D **100**, 023011 (2019).

[86] T. Venumadhav, B. Zackay, J. Roulet, L. Dai, and M. Zaldarriaga, New Binary Black Hole Mergers in the Second Observing Run of Advanced LIGO and Advanced Virgo, arXiv e-prints , arXiv:1904.07214 (2019), arXiv:1904.07214 [astro-ph.HE].

[87] B. Zackay, L. Dai, T. Venumadhav, J. Roulet, and M. Zaldarriaga, Detecting Gravitational Waves With Disparate Detector Responses: Two New Binary Black Hole Mergers, arXiv e-prints , arXiv:1910.09528 (2019), arXiv:1910.09528 [astro-ph.HE].

[88] B. P. Abbott, R. Abbott, T. D. Abbott, *et al.*, GWTC-2: Compact Binary Coalescences Observed by LIGO and Virgo During the First Half of the Third Observing Run, arXiv e-prints , arXiv:2010.14527 (2020), arXiv:2010.14527 [gr-qc].

[89] Q. Chu, M. Kovalam, L. Wen, T. Slaven-Blair, and et al., The SPIIR online coherent pipeline to search for gravitational waves from compact binary coalescences, arXiv e-prints , arXiv:2011.06787 (2020), arXiv:2011.06787 [gr-qc].

[90] S. Sachdev, S. Caudill, H. Fong, R. K. Lo, C. Messick, D. Mukherjee, R. Magee, L. Tsukada, K. Blackburn, P. Brady, *et al.*, The GstLAL Search Analysis Methods for Compact Binary Mergers in Advanced LIGO's Second and Advanced Virgo's First Observing Runs, arXiv preprint arXiv:1901.08580 (2019).

[91] S. Klimenko, G. Vedovato, M. Drago, F. Salemi, V. Tiwari, G. A. Prodi, C. Lazzaro, K. Ackley, S. Tiwari, C. F. Da Silva, and G. Mitselmakher, Method for detection and reconstruction of gravitational wave transients with networks of advanced detectors, Phys. Rev. D **93**, 042004 (2016).

[92] R. Abbott, T. D. Abbott, S. Abraham, F. Acernese, and et al., (2020).

[93] G. Ashton, M. Hübner, P. Lasky, and C. Talbot, Bilby: A User-Friendly Bayesian Inference Library (2019).

[94] G. Ashton, I. Romero-Shaw, C. Talbot, C. Hoy, and S. Galaudage, bilby pipe: 1.0.1 (2020).

[95] J. S. Speagle, DYNESTY: a dynamic nested sampling package for estimating Bayesian posteriors and evidences, MNRAS **493**, 3132 (2020), arXiv:1904.02180 [astro-ph.IM].

[96] J. Skilling, Nested Sampling, in *Bayesian Inference and Maximum Entropy Methods in Science and Engineering: 24th International Workshop on Bayesian Inference and Maximum Entropy Methods in Science and Engineering*, American Institute of Physics Conference Series, Vol. 735, edited by R. Fischer, R. Preuss, and U. V. Toussaint (2004) pp. 395–405.

[97] J. Skilling, Nested sampling for general Bayesian computation, Bayesian Analysis **1**, 833 (2006).

[98] G. Ashton, M. Hübner, P. D. Lasky, C. Talbot, K. Ackley, S. Biscoveanu, Q. Chu, A. Divakarla, P. J. Easter, B. Goncharov, F. Hernandez Vivanco, J. Harms, M. E. Lower, G. D. Meadors, D. Melchor, E. Payne, M. D. Pitkin, J. Powell, N. Sarin, R. J. E. Smith, and E. Thrane, BILBY: A User-friendly Bayesian Inference Library for Gravitational-wave Astronomy, ApJS **241**, 27 (2019), arXiv:1811.02042 [astro-ph.IM].

[99] R. J. E. Smith, G. Ashton, A. Vajpeyi, and C. Talbot, Massively parallel Bayesian inference for transient gravitational-wave astronomy, MNRAS **498**, 4492 (2020), arXiv:1909.11873 [gr-qc].

[100] E. Thrane and C. Talbot, An introduction to Bayesian inference in gravitational-wave astronomy: Parameter estimation, model selection, and hierarchical models, PASA **36**, e010 (2019), arXiv:1809.02293 [astro-ph.IM].

[101] I. M. Romero-Shaw, C. Talbot, S. Biscoveanu, V. D'Emilio, G. Ashton, *et al.*, Bayesian inference for compact binary coalescences with BILBY: validation and application to the first LIGO-Virgo gravitational-wave transient catalogue, MNRAS **499**, 3295 (2020), arXiv:2006.00714 [astro-ph.IM].

[102] J. Veitch, V. Raymond, B. Farr, W. Farr, and et al., Parameter estimation for compact binaries with ground-based gravitational-wave observations using the LALInference software library, Phys. Rev. D **91**, 042003 (2015), arXiv:1409.7215 [gr-qc].

[103] S. Khan, S. Husa, M. Hannam, F. Ohme, M. Pürrer, X. J. Forteza, and A. Bohé, Frequency-domain gravitational waves from nonprecessing black-hole binaries. II. A phenomenological model for the advanced detector era, Physical Review D **93**, 044007 (2016).

[104] G. Pratten, C. García-Quirós, M. Colleoni, A. Ramos-Buades, and et al., Computationally efficient models for the dominant and sub-dominant harmonic modes of precessing binary black holes, arXiv e-prints , arXiv:2004.06503 (2020), arXiv:2004.06503 [gr-qc].

[105] J. Blackman, S. E. Field, M. A. Scheel, C. R. Galley, C. D. Ott, M. Boyle, L. E. Kidder, H. P. Pfeiffer, and B. Szilágyi, Numerical relativity waveform surrogate model for generically precessing binary black hole mergers, Phys. Rev. D **96**, 024058 (2017), arXiv:1705.07089 [gr-qc].

[106] S. Ossokine, A. Buonanno, S. Marsat, R. Cotesta, S. Babak, T. Dietrich, R. Haas, I. Hinder, H. P. Pfeiffer, M. Pürrer, C. J. Woodford, M. Boyle, L. E. Kidder, M. A. Scheel, and B. Szilágyi, Multipolar effective-one-body waveforms for precessing binary black holes: Construction and validation, Phys. Rev. D **102**, 044055 (2020), arXiv:2004.09442 [gr-qc].

[107] B. P. Abbott, R. Abbott, T. D. Abbott, *et al.*, A guide to LIGO-Virgo detector noise and extraction of transient gravitational-wave signals, arXiv e-prints , arXiv:1908.11170 (2019), arXiv:1908.11170 [gr-qc].

[108] C. Talbot and E. Thrane, Gravitational-wave astronomy with an uncertain noise power spectral density, arXiv e-prints , arXiv:2006.05292 (2020), arXiv:2006.05292 [astro-ph.IM].

[109] K. Chatziioannou, C.-J. Haster, T. B. Littenberg, W. M. Farr, S. Ghonge, M. Millhouse, J. A. Clark, and N. Cornish, Noise spectral estimation methods and their impact on gravitational wave measurement of compact binary mergers, Phys. Rev. D **100**, 104004 (2019).

[110] S. Biscoveanu, C.-J. Haster, S. Vitale, and J. Davies, Quantifying the effect of power spectral density uncertainty on gravitational-wave parameter estimation for compact binary sources, Phys. Rev. D **102**, 023008 (2020), arXiv:2004.05149 [astro-ph.HE].

[111] R. Abbott, T. D. Abbott, S. Abraham, F. Acernese, and et al., Open data from the first and second observing runs of Advanced LIGO and Advanced Virgo, SoftwareX **13**, 100658 (2021), arXiv:1912.11716 [gr-qc].

[112] D. Macleod, A. L. Urban, S. Coughlin, T. Massinger, M. Pitkin, paulaltin, J. Areeda, E. Quintero, T. G. Badger, L. Singer, and K. Leinweber, gwpy/gwpy: 1.0.1 (2020).

[113] S. Galaudage, C. Talbot, and E. Thrane, Gravitational-wave inference in the catalog era: Evolving priors and marginal events, Phys. Rev. D **102**, 083026 (2020), arXiv:1912.09708 [astro-ph.HE].

[114] A. H. Nitz, C. D. Capano, S. Kumar, Y.-F. Wang, S. Kastha, M. Schäfer, R. Dhurkunde, and M. Cabero, 3-OGC: Catalog of gravitational waves from compact-binary mergers, arXiv e-prints , arXiv:2105.09151 (2021), arXiv:2105.09151 [astro-ph.HE].

[115] S. E. Woosley and A. Heger, The Pair-Instability Mass Gap for Black Holes, arXiv e-prints , arXiv:2103.07933 (2021), arXiv:2103.07933 [astro-ph.SR].

[116] A. Heger and S. E. Woosley, The Nucleosynthetic Signature of Population III, ApJ **567**, 532 (2002), arXiv:astro-ph/0107037 [astro-ph].

[117] Carbonfund.org, Carbon Fund (2020).

[118] Gravitational Wave Open Science Center, The O2 Data Release, `https://doi.org/10.7935/CA75-FM95`.

[119] LIGO Scientific Collaboration, LIGO Algorithm Library - LALSuite, free software (GPL) (2018).

[120] J. D. Hunter, Matplotlib: A 2d graphics environment, Computing in science & engineering **9**, 90 (2007).

[121] C. R. Harris, K. J. Millman, S. J. van der Walt, R. Gommers, P. Virtanen, D. Cournapeau, E. Wieser, J. Taylor, S. Berg, N. J. Smith, R. Kern, M. Picus, S. Hoyer, M. H. van Kerkwijk, M. Brett, A. Haldane, J. Fernández del Río, M. Wiebe, P. Peterson, P. Gérard-Marchant, K. Sheppard, T. Reddy, W. Weckesser, H. Abbasi, C. Gohlke, and T. E. Oliphant, Array programming with NumPy, Nature **585**, 357–362 (2020).

[122] P. Virtanen, R. Gommers, T. E. Oliphant, M. Haberland, T. Reddy, D. Cournapeau, E. Burovski, P. Peterson, W. Weckesser, J. Bright, S. J. van der Walt, M. Brett, J. Wilson, K. J. Millman, N. Mayorov, A. R. J. Nelson, E. Jones, R. Kern, E. Larson, C. J. Carey, İ. Polat, Y. Feng, E. W. Moore, J. VanderPlas, D. Laxalde, J. Perktold, R. Cimrman, I. Henriksen, E. A. Quintero, C. R. Harris, A. M. Archibald, A. H. Ribeiro, F. Pedregosa, P. van Mulbregt, and SciPy 1.0 Contributors, SciPy 1.0: Fundamental Algorithms for Scientific Computing in Python, Nature Methods **17**, 261 (2020).

[123] T. pandas development team, pandas-dev/pandas: Pandas (2020).

[124] T. E. Oliphant, Python for scientific computing, Computing in Science Engineering **9**, 10 (2007).

[125] K. J. Millman and M. Aivazis, Python for scientists and engineers, Computing in Science Engineering **13**, 9 (2011).